Precision Mechanics & Digital Fabrication
https://www.acadlore.com/journals/PMDF

Influence of Rotation Step Size on Incident Solar Irradiance in Flat-Plate Collectors with Single-Axis Tracking Under Clear-Sky Conditions

Aleksandar Nešović[1*], Igor Saveljić[2]

[1] Scientific Research Center for the Application of Information Technologies in Engineering, Institute for Information Technologies Kragujevac, University of Kragujevac, 34000 Kragujevac, Serbia
[2] Scientific Research Center for Numerical Modeling and Biomechanics, Institute for Information Technologies Kragujevac, University of Kragujevac, 34000 Kragujevac, Serbia

[*] Correspondence: Aleksandar Nešović (aca.nesovic@kg.ac.rs)

Received: 03-26-2025 **Revised:** 05-14-2025 **Accepted:** 05-20-2025

Citation: A. Nešović and I. Saveljić, "Influence of rotation step size on incident solar irradiance in flat-plate collectors with single-axis tracking under clear-sky conditions," *Precis. Mech. Digit. Fabr.*, vol. 2, no. 2, pp. 83–92, 2025. https://doi.org/10.56578/pmdf020202.

Abstract: The effectiveness of single-axis solar tracking in enhancing the performance of flat-plate solar collectors (FPSCs) has been widely acknowledged, particularly under clear-sky conditions. However, the precision of solar tracking systems—governed by the electro-mechanical transmission's discrete rotation step size—has a critical impact on energy yield. In this study, the influence of varying rotation step sizes on the incident solar irradiance received by flat-plate collectors with single-axis tracking (SAT) has been numerically investigated using the EnergyPlus simulation environment. Eight discrete step sizes—1°, 2°, 5°, 10°, 15°, 30°, 45°, and 90°—were examined under clear-sky conditions on July 26, using meteorological data specific to Kragujevac, Serbia. The tracking system was configured to follow the solar trajectory along the east–west (E–W) direction, rotating around a north–south (N–S) inclined axis. Results demonstrated that incident solar irradiance was significantly enhanced—by over 35%—when rotation step sizes ranged between 1° and 15°, compared to fixed (non-tracking) collectors. Slight reductions in performance were observed for step sizes of 30° (34.26% improvement) and 45° (32.95%), with the lowest gain (23.04%) associated with the coarsest resolution of 90°. Although dual-axis tracking (DAT) systems provide superior irradiance capture, single-axis systems offer substantial advantages in residential and small-scale applications due to their lower capital investment, simpler design, reduced maintenance requirements, and greater architectural integration potential. These findings underscore the importance of optimizing rotation step size in the design and deployment of cost-effective, energy-efficient solar tracking systems. In light of increasingly stringent energy performance directives within the European Union, the deployment of optimally configured SAT systems is expected to expand across the residential sector.

Keywords: Clear-sky conditions; Flat-plate solar collector (FPSC); Incident solar irradiance; Numerical simulation; Rotation step size; Single-axis tracking (SAT); Solar energy optimization

1 Introduction

All solar systems, depending on their purpose, can be classified into three large groups: solar thermal collectors [1] convert solar energy into thermal energy, photovoltaic panels [2] convert solar energy into electricity and photovoltaic-thermal collectors [3] convert solar energy into thermal energy and electricity at the same time.

Regardless of their purpose, all solar systems can be classified, or into the non-tracking (fixed) [4] group, or into the tracking [5] group.

Among other things, the global scientific community has defined several sub-criteria for the classification of tracking solar systems [6–14]: control strategy (closed-loop, open-loop, hybrid), drive unit (active, passive), degree of freedom (SAT, DAT, Table 1) and strategy method (sensor, date and time, combined).

In the available literature, FPSC with tracking mechanisms, both SAT and DAT, were the subject of theoretical, numerical, experimental and combined research.

Table 1. Performance of the tracking solar collectors [15, 16]

Parameter	SAT	DAT
Mechanism	Simple	Complicated
Degree of freedom	One	Two
Rotation axis	Horizontal, vertical, inclined, combined	Combined
Rotation direction	E-W, N-S	Combined
Setup cost	Cheap	Also costly
Running cost	Low	High
Measuring movement	Vertical	Vertical and horizontal
Average efficiency compared with fixed solar collector	30% higher	40% higher

Neville [17] developed and presented two mathematical models. First, for describing the thermal performance of the FPSC with SAT, and the second one for describing the thermal performance of the FPSC with DAT. The results of the theoretical research presented by Drago [18] demonstrated the justification of the DAT concept, as this approach can improve thermal efficiency by over 20%. Thomson and Tamm [19, 20] compared the fixed FPSC and the FPSC with DAT. The results of theoretical and experimental research, in the climatic conditions of Estonia (city of Tallinn), indicated that the seasonal energy yield in the case of the tracking solar collector is higher by 10-20%. Depending on the tracking concept, FPSCs can reach the following thermal efficiency values [21]: 57.12% (sun tracking in the N-S direction around the E-W horizontal rotation axis), 62.17% (sun tracking in the E-W direction around the N-S horizontal rotation axis), 59.51% (sun tracking in the E-W direction around the vertical rotation axis), 64.36% (sun tracking in the E-W direction around the N-S inclined rotation axis) and 67.25% (sun tracking with two degrees of freedom). Different approaches in creating mathematical models for the fixed and tracking solar collectors can be found in references [22–24]. A review paper that, among other things, took into account the economic aspects of tracking FPSCs was presented in Bahrami et al. [25]. The isotropic and anisotropic diffuse (ground albedo and clouds effects) models to estimate the total solar energy received on the fixed and tracking (DAT) FPSCs are theoretically investigated by Kambezidis et al. [26].

The algorithm for adaptive tracking for FPSCs with experimental validation was developed by Neagoe et al. [27]. Their model was based on the new concept that considers inverse tracking as a viable option for protecting the collectors against overheating. For weather conditions in the city of Shtip (Northern Macedonia), Chekerovska and Filkoski experimentally (along with the development and verification of the 3D mathematical model) investigated the Sun tracking effect on the FPSC efficiency [28]. An interesting numerical study (using TRNSYS software) was conducted by Ajunwa et al. [29]. The subject of their study was an FPSC intended for solar drying. The solar collector was equipped with two side reflectors (on the east and west sides) and a manual SAT mechanism. The position of the reflectors could also be adjusted. The authors determined the optimal positions of the west and east reflectors for three months, respectively: 80° and 45° (for January), 80° and 40° (for February and March). Using the manual SAT mechanism, the total percentage of moisture loss increased by 5.11%.

This paper discusses the use of the EnergyPlus software in thermal analyses of solar tracking systems. The mentioned software is not primarily intended for such simulations because it does not have the appropriate tools. This numerical investigation continues the papers presented by Nešović et al. [30, 31], where the research subject was the FPSC with a specific SAT mechanism, more precisely, the FPSCs with SAT tracking in the E-W direction around the N-S rotation axis. For a specific location in Central Serbia (the city of Kragujevac), meteorological data for July 26 were used to determine the relationship between different rotation steps and incident solar radiation during one clear-sky day. Specifically, 8 different tracking scenarios (1°, 2°, 5°, 10°, 15°, 30°, 45° and 90°) were considered in this case. The obtained results are also compared with the performance of the fixed FPSC, which had a controlling role.

2 Materials and Methods

Geometric characteristics of the FPSC and main elements of the electro-mechanical transmission in the adopted tracking mechanism are described in Section 2.1. In Section 2.2, meteorological data (incident solar radiation on a horizontal surface, air temperature and wind speed) for the city of Kragujevac during July 26 are presented. The last sections are dedicated to the used software: Google SketchUp (Section 2.3) and EnergyPlus (Section 2.4).

2.1 Subject Research

Figure 1 shows the FPSC's geometry designed in Google SketchUp software. The collector dimensions are 500×800 mm, meaning the collector surface is less than 0.5 m^2. The optimal inclination angle (in the N-S direction) of the solar collector to the horizontal for the city of Kragujevac (β=34°) was determined according to the recommendations from reference [32]. The lower edge is located at a height of 700 mm from the ground. The given data determine the neutral position of the solar collector in space (Figure 1).

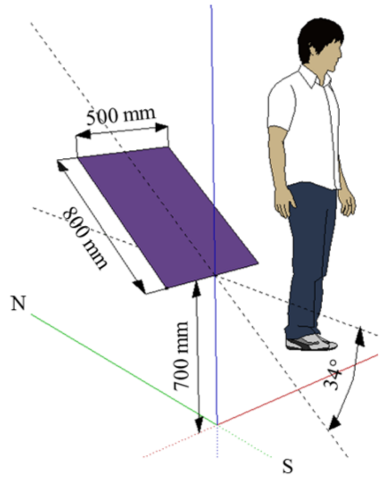

Figure 1. Isometric view of the FPSC in neutral position

The FPSC is equipped with a specific SAT mechanism. Namely, sun tracking in the E-W direction around the N-S inclined rotation axis is enabled by the use of electro-mechanical transmission. The components of the mechanical transmission are shown in Figure 2, while the components of the electric transmission are shown in Figure 3.

The role of the drive unit, on which the drive chain is located, is played by the hybrid stepper servo motor (Figure 2). The stepper motor is placed under the FPSC. The planetary reducer enables a wide range of rotation step settings (its primary role). The torque, rotation step and mechanical power are transmitted from the drive chain to the chased sprocket via a chain transmission. The driven sprocket is integrated with the FPSC.

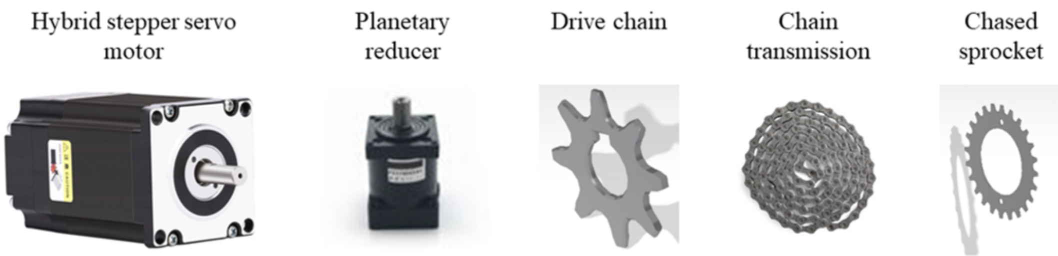

Figure 2. Main elements of the mechanical transmission

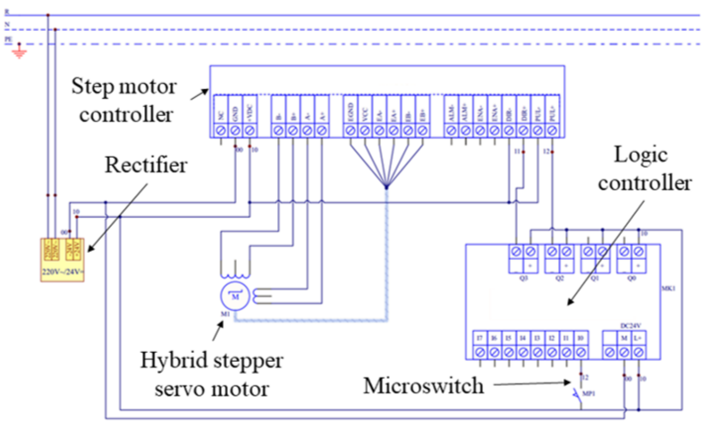

Figure 3. Main elements of the electrical transmission

The role of the main executive element, during the day, has a microswitch. The microswitch operation is controlled by a logic controller with a predefined date and time schedule. The logic controller determines the stepper motor operation within the layout itself via the stepper motor controller.

2.2 Meteorological Data

Total H_{tot} $\left[\mathrm{W.m^{-2}}\right]$, beam H_{beam} $\left[\mathrm{W.m^{-2}}\right]$ and diffuse H_{diff} $\left[\mathrm{W.m^{-2}}\right]$ terrestrial solar radiation on the horizontal surface located in the city of Kragujevac ($\varphi = 44.02°\mathrm{N}$ and $\lambda = 20.92°\mathrm{E}$) during July 26 are shown in Figure 4.

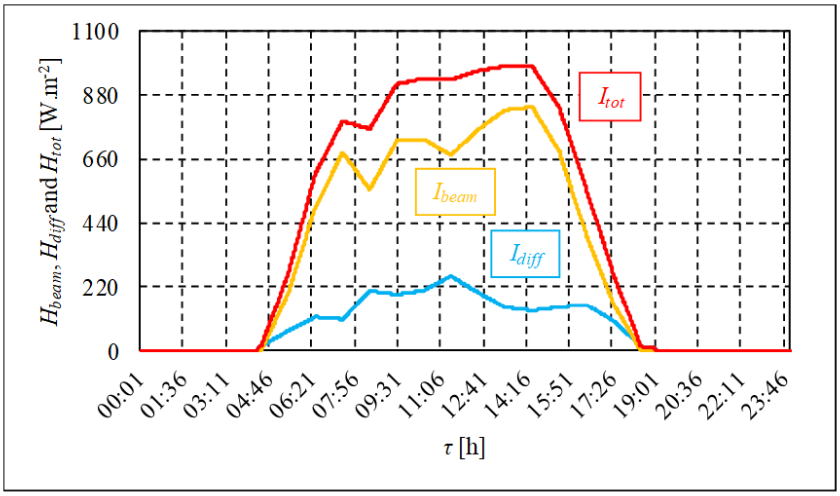

Figure 4. Terrestrial solar radiation on a horizontal surface during July 26 [33]

For July 26 (clear day, sunrise at 04:23 h, sunset at 19:03 h), the following average daily values were measured (Figure 4): $H_{tot,avg} = 667.61\ \mathrm{W\cdot m^{-2}}$, $H_{beam,avg} = 525.83\ \mathrm{W\cdot m^{-2}}$ and $H_{diff,avg} = 141.78\ \mathrm{W\cdot m^{-2}}$. The maximum values were recorded at 13:30 h $\left(H_{tot,max} = 978\ \mathrm{W\cdot m^{-2}}\right)$, $14:30$ h $\left(H_{beam,max} = 838\ \mathrm{W\cdot m^{-2}}\right)$ and $11:30$ h $\left(H_{diff,\,max} = 258\ \mathrm{W\cdot m^{-2}}\right)$. The cloudy-sky periods (which can be concluded from the discontinuity of the terrestrial beam solar radiation curve) are present in the period from 07:30 h to 15:00 h.

During the mentioned period for the analyzed location, the wind speed $c_w\left[\mathrm{m\cdot s^{-1}}\right]$ (Figure 5) is variable, but it is within the limits between $c_{w,min} = 0.4\ \mathrm{m\cdot s^{-1}}$(07:00 h) and $c_{w,max} = 3.1\ \mathrm{m\cdot s^{-1}}$(17:00 h). Average daily air temperature is $t_{o,avg}$=21.81℃ (Figure 5). Minimum and maximum daily values are $t_{o,min}$=19.1℃ (04:00 h) and $t_{o,max}$=24.7℃ (15:00 h), respectively.

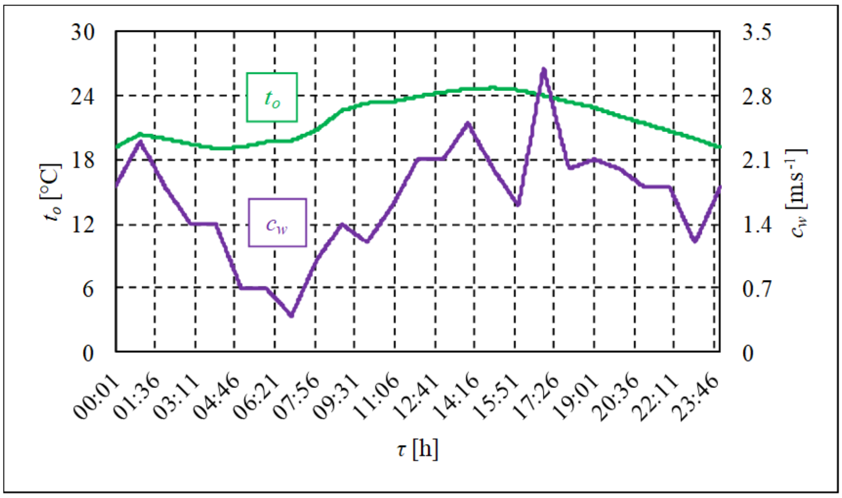

Figure 5. Air temperature and wind speed during July 26 [33]

2.3 Google SketchUp Software

Google SketchUp software is primarily intended for the 3D modeling of buildings [34]. The interface provides faster and simpler work compared to other similar software. Models with a large number of details (shading elements, daylighting control, etc.) can be created in this software. It also provides many other possibilities, such as integration with Google Earth services and EnergyPlus software. Communication with EnergyPlus software is enabled by 2 tool palettes: Legacy OpenStudio and Legacy OpenStudio Rendering.

2.4 EnergyPlus Software

The EnergyPlus software is intended for numerical investigations of energy and ecological communication between buildings and the environment [35]. It was developed by Lawrence Berkeley, the National Laboratory, the US Army Construction Engineering Laboratory, and the University of Illinois [36]. The software is used in various thermo-technical analyses: heating, cooling, air conditioning, ventilation, solar systems, etc.

3 Scenario Simulations

Since there are no models for analyzing tracking solar systems in the EnergyPlus software, the models were artificially created for the purposes of this study.

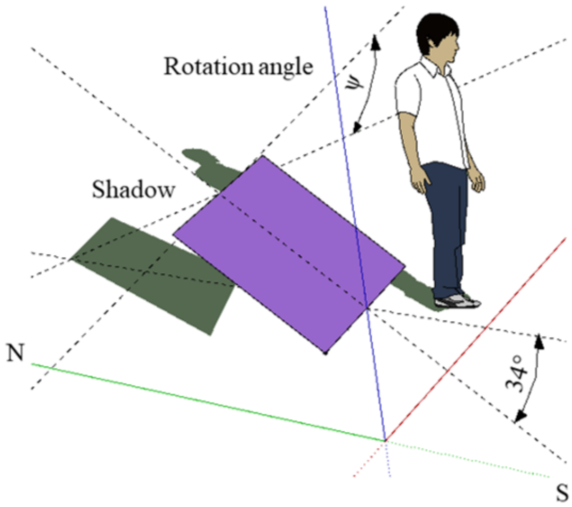

Figure 6. Isometric view of the FPSC in working mode

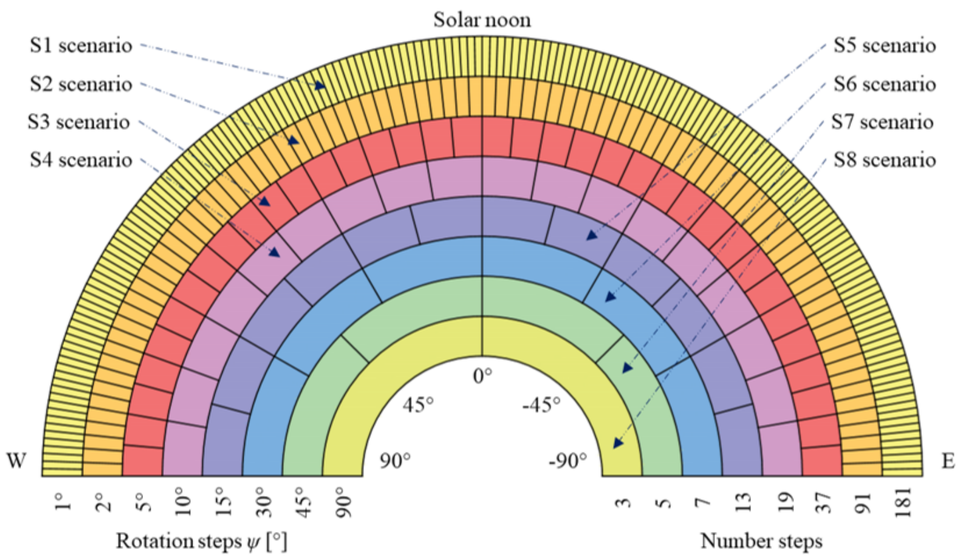

Figure 7. Scenario simulations

Namely, through a series of simulations, the total incident solar radiation was calculated during the day, for each FPSC rotation angle in the E-W direction around the inclined N-S rotation axis (Figure 6): from -90° (the moment of sunrise) to +90° (the moment of sunset). The rotation angle was 1°. For the results to be as accurate as possible, the one-minute time step was used (Figure 4 and Figure 5). The maximum numerical value for each rotation angle at a given time was used to form the daily curve of total incident solar radiation. In this way, a large database was created, which was then used to create different tracking scenarios, in this particular case, based on 8 rotation steps $\psi\,[^\circ] : \psi = 1^\circ, \psi = 2^\circ, \psi = 5^\circ, \psi = 10^\circ, \psi = 15^\circ, \psi = 30^\circ, \psi = 45^\circ$ and $\psi = 90^\circ$. All analyzed cases are graphically presented in Figure 7.

Total incident solar radiation I_{tot} [W] on the tracking surface, i.e., FPSC with SAT, is determined by Eq. (1):

$$I_{tot} = I_{beam} + I_{diff} + I_{refl} \tag{1}$$

where, I_{beam} [W] is the beam incident solar radiation, I_{diff} [W] is the diffuse incident solar radiation Eq. (2) and I_{refl} [W] is the reflected incident solar radiation Eq. (3) [37].

$$I_{diff} = I_{diff,cr} + I_{diff,sd} + I_{diff,sh} \tag{2}$$

$$I_{refl} = I_{refl,\ beam} + I_{refl,\ diff} \tag{3}$$

where, $I_{diff,\ cr}$ [W] is the diffuse incident solar radiation from the circumsolar region, $I_{diff,\ sd}$ [W] is the diffuse incident solar radiation from the sky dome, $I_{diff,\ sh}$ [W] is the diffuse incident solar radiation from the sky horizon, $I_{refl,\ beam}$ [W] is the reflected beam incident solar radiation and $I_{refl,\ diff}$ [W] is the reflected diffuse incident solar radiation [37].

4 Results and Discussion

In the following diagram (Figure 8), firstly are shown the numerical results of the average daily total incident solar radiation $I_{tot,avg}\,[\mathrm{W.\ day}^{-1}]$ on the fixed FPSC for some cases of the angle $\psi_{fix}\,[^\circ]$. The results are based on the use of meteorological data for the city of Kragujevac during July 26, which was already mentioned in Sub-section 2.2. In all analyzed cases, the angle $\beta = 34^\circ$ is the same. The angle $\psi_{fix} = -90^\circ$ refers to the solar collector that is completely facing east during the day. When $\psi_{fix} = 0^\circ$, the solar collector is oriented towards the south during the day, which means that in the case of $\psi_{fix} = 90^\circ$ it is completely facing west.

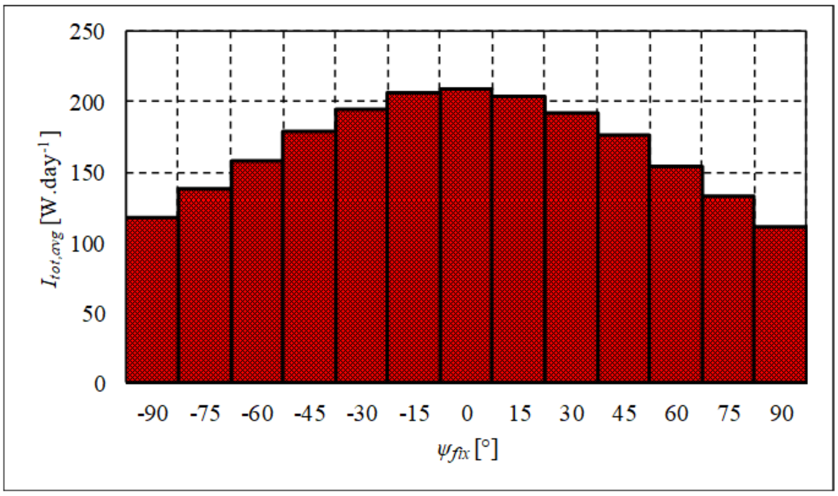

Figure 8. Total average incident solar radiation on the fixed FPSC depending on the rotation angles during July 26

As shown in Figure 8, $I_{tot,avg}$ value is the highest when the fixed FPSC is oriented towards the south at an angle of $\beta = 34^\circ$ ($I_{tot,avg} = 209.24$ W. day $^{-1}$). In cases where $\psi_{fix} = -90^\circ$ and $\psi_{fix} = 90^\circ$, this value is reduced 1.78 times $\left(I_{tot,\ avg} = 117.55\ \mathrm{W.day}^{-1}\right)$ and 1.86 times $\left(I_{tot,\ avg} = 110.83\ \mathrm{W.day}^{-1}\right)$.

The orientation of the FPSC primarily affects the component $I_{beam,\ avg}\,[\mathrm{W.\ day}^{-1}]$, because it is directly related to the solar incident angle [38]. Since the component $I_{diff,\ avg}\,[\mathrm{W.\ day}^{-1}]$ originates from three sources (Section 3), its share in $I_{tot,\ avg}\,[\mathrm{W.\ day}^{-1}]$ is much smaller and can be neglected in some cases. For the sake of comparison, the option $\psi_{fix} = -60^\circ$ is 34.86% better than $\psi_{fix} = -90^\circ$, but also 24.24% worse than $\psi_{fix} = 0^\circ$. The diagram shown in Figure 7 actually proves that the southern orientation of the fixed FPSC is the optimal solution.

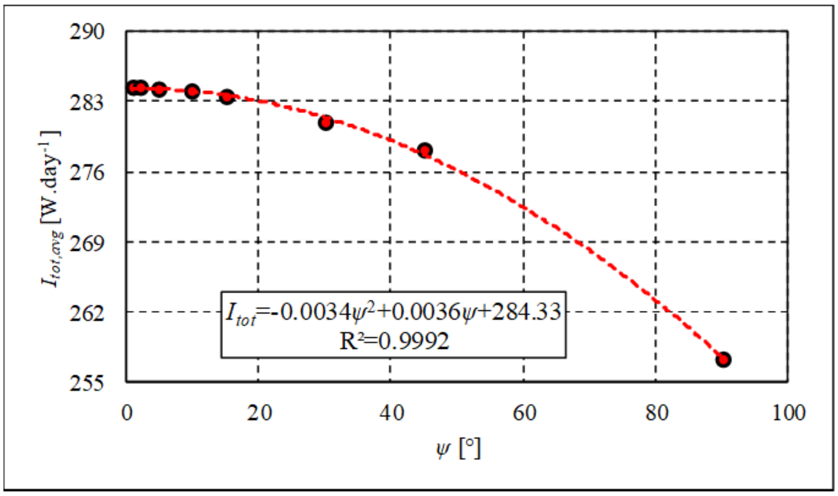

Figure 9. Functional dependence between the total average incident solar radiation on the FPSC and rotation steps during July 26

Table 2. Total average incident solar radiation on the different tracking FPSCs during July 26

ψ [°]	1	2	5	10	15	30	45	90
$I_{tot,avg}$ [W . day $^{-1}$]	284.41	284.4	284.26	284.06	283.53	280.92	278.18	257.45

The comparison of all 8 adopted tracking scenarios (Section 3, Figure 7) through the $I_{tot,avg}$ indicator during the same day (July 26) is shown in Figure 9 and Table 2.

If the mentioned values $I_{tot,avg}$ for FPSC with different rotation steps (Figure 9), are compared with the value $I_{tot,avg}$ for $\psi_{fix} = 0°$ (Figure 8), i.e., FPSC, the following SAT mechanism benefits can be seen: 35.923% for ($\psi = 1°$), 35.918% (for $\psi = 2°$), 35.85% (for $\psi = 5°$), 35.75% (for $\psi = 10°$), 35.51% (for $\psi = 15°$), 34.26% (for $\psi = 30°$), 32.95% (for $\psi = 45°$) and 23.04% (for $\psi = 90°$).

The next diagram (Figure 10) shows the I_{tot}[W] values, both for the fixed FPSC ($\psi_{fix} = 0°$) and for some cases tracking FPSC ($\psi = 1°, \psi = 30°, \psi = 45°$ and $\psi = 90°$). Solar radiation curves, from sunrise to sunset (July 26), were created based on a sample with a one-minute measurement step.

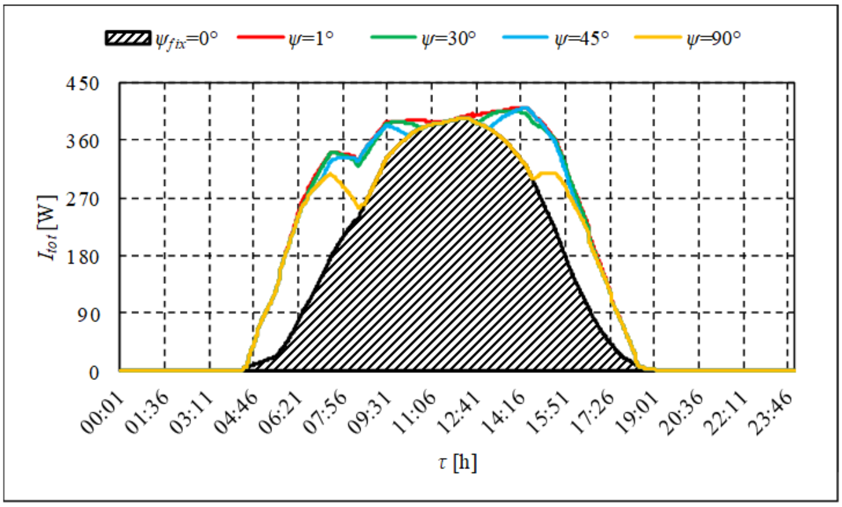

Figure 10. Total incident solar radiation on the tracking FPSC depending on the rotation steps during July 26

The first thing that can be seen from Figure 10 is that the rotation step increases the area under the solar curve. Thus, for example, the area under the solar curve ψ=90° is greater than the area corresponding to the solar curve ψ_{fix}=0°. The area under the solar curve ψ=1° is the largest, which is according to the Itot,avg values ($I_{tot,avg}$=284.41 W . day^{-1}). Figure 10 also shows that the solar curves overlap to some extent during the day: ψ=90° and ψ_{fix}=0° (for example, between 08:44 h and 14:41 h), ψ=1°, ψ=30°, ψ=45° and ψ=90° (for example, between sunrise and 06:14 h), etc. Another interesting effect can be observed from Figure 10, which is that there is a short period during the day when all the solar curves are tangent to each other. It is the period of solar noon (11:43 h). Then the sun is at its zenith (maximum altitude angle $\alpha_{\max}$=65.58°) for the analyzed day (in this case, July 26), so the solar incident angle is the same for all solar structures, regardless of whether the tracking mechanism is applied or not, regardless of the applied rotation step.

Tanging also occurs when the I_{tot} value decreases, that is, due to the reduction of the I_{beam} (moments of cloudiness, between 07:56 h and 09:31 h, Figure 10). Then the power of the solar collector for $\psi = 90°$ is close to the power of the solar collector for $\psi = 0°$, and the same phenomenon occurs at $\psi = 1°, \psi = 30°$ and $\psi = 45°$. This means that weather conditions affect the energy performance of tracking solar collectors.

In relation to $\psi_{fix} = 0°$, the greatest benefits in the case of using $\psi = 90°$ are achieved in the morning and evening hours, concretely at 06:30 h (I_{tot} is higher for 166.62 W). The advantage of using the remaining rotation steps ($\psi = 1°$, $\psi = 30°$ and $\psi = 45°$) in relation to $\psi = 90°$ is achieved precisely between the mentioned (morning and evening) periods and the moment of solar noon (Figure 10): $\psi = 45°$ (I_{tot} is higher for 102.76 W, 14:40 h), $\psi = 30°$ (I_{tot} is higher for 89.09 W, 14:41 h) and $\psi = 1°$ (I_{tot} is higher for 101.98 W, 14:39 h).

5 Conclusions

In this paper, the numerical method (tool) was applied to analyze the thermal performance of the FPSC with a specific tracking mechanism (SAT in the E-W direction around the N-S inclined rotation axis). For this purpose, the following software was used: Google SketchUp (for defining the geometry) and EnergyPlus (for conducting simulations). The simulations were conducted using weather data for the city of Kragujevac. The main goal of the paper was to determine the functional dependence between different rotation steps (1°, 2°, 5°, 10°, 15°, 0°, 45° and 90°) and incident solar radiation for a selected location during one clear-sky day (July 26). The control role is assigned to the fixed FPSC. All solar collectors (tracking and fixed) had the same inclination angle to the horizontal (34°).

Results showed that the total average incident solar radiation for the fixed FPSC is 209.24 W.day^{-1}. The same parameter in the case of the tracking FPSCs ranged between 257.45 W.day^{-1} (for 90°) and 284.41 W.day^{-1} (for 1°). In comparison with the fixed FPSC, the percentage benefits of the tracking FPSC were between 23.04-35.923%.

Taking into account adopted location parameters, investment costs, weather parameters that can be variable, as well as simulation results, the general practical recommendation is that a rotation step smaller than 15° has no practical sense because the impact on the total average incident solar radiation is almost negligible.

Following the research results, additional numerical simulations of the SAT solar collectors will be conducted in the coming period. They will take into account different locations in Serbia (1) and incident solar radiation in variable meteorological conditions, such as days with extremely clear-sky and cloudy-sky days (2).

Author Contributions

Conceptualization, A.N. and I.S.; methodology, A.N. and I.S.; software, A.N.; validation, I.S.; formal analysis, A.N. and I.S.; investigation, A.N.; resources, I.S.; data curation, A.N. and I.S.; writing—original draft preparation, A.N.; writing—review and editing, I.S.; visualization, A.N.; supervision, I.S. All authors have read and agreed to the published version of the manuscript.

Data Availability

Not applicable.

Conflicts of Interest

The authors declare no conflict of interest.

References

[1] Y. Tian and C. Y. Zhao, "A review of solar collectors and thermal energy storage in solar thermal applications," *Appl. Energy*, vol. 104, pp. 538–553, 2013. https://doi.org/10.1016/j.apenergy.2012.11.051

[2] S. A. Rahman, R. K. Varma, and T. Vanderheide, "Generalised model of a photovoltaic panel," *IET Renew. Power Gener.*, vol. 8, no. 3, pp. 217–229, 2014. https://doi.org/10.1049/iet-rpg.2013.0094

[3] S. B. Riffat and E. Cuce, "A review on hybrid photovoltaic/thermal collectors and systems," *Int. J. Low-Carbon Technol.*, vol. 6, no. 3, pp. 212–241, 2011. https://doi.org/10.1093/ijlct/ctr016

[4] J. D. Garrison, "Optimization of a fixed solar thermal collector," *Sol. Energy*, vol. 23, no. 2, pp. 93–102, 1979. https://doi.org/10.1016/0038-092X(79)90108-7

[5] S. Racharla and K. Rajan, "Solar tracking system–A review," *Int. J. Sustain. Eng.*, vol. 10, no. 2, pp. 72–81, 2017.

[6] J. L. Pérez-Gudiño, M. A. Gómez-Guzmán, C. García-Valdez, R. V. Carrillo-Serrano, G. I. Pérez-Soto, and J. Rodríguez-Reséndiz, "The low-cost mechanism of a defined path guide slot-based passive solar tracker intended for developing countries," *Technologies*, vol. 12, no. 12, p. 250, 2024. https://doi.org/10.3390/technologies12120250

[7] K. Kumba, P. Upender, P. Buduma, M. Sarkar, S. P. Simon, and V. Gundu, "Solar tracking systems: Advancements, challenges, and future directions: A review," *Energy Rep.*, vol. 12, pp. 3566–3583, 2024. https://doi.org/10.1016/j.egyr.2024.09.038

[8] N. Kuttybay, S. Mekhilef, N. Koshkarbay, A. Saymbetov, M. Nurgaliyev, G. Dosymbetova, S. Orynbassar, E. Yershov, A. Kapparova, B. Zholamanov, and A. Bolatbek, "Assessment of solar tracking systems: A comprehensive review," *Sustain. Energy Technol. Assessments*, vol. 68, p. 103879, 2024. https://doi.org/10.1016/j.seta.2024.103879

[9] A. Priyam, "Solar tracking systems–A review," *J. Mines Met. Fuels.*, vol. 71, no. 10, pp. 1725–1736, 2023. https://doi.org/10.18311/jmmf/2023/35863

[10] A. Awasthi, A. K. Shukla, S. R. Murali Manohar, C. Dondariya, K. N. Shukla, D. Porwal, and G. Richhariya, "Review on sun tracking technology in solar PV system," *Energy Rep.*, vol. 6, pp. 392–405, 2020. https://doi.org/10.1016/j.egyr.2020.02.004

[11] A. Nešović, N. Lukić, R. Kowalik, A. Janaszek, D. Taranović, and Koz lowski, T., "Experimental and numerical comparison of glass tube collector with relative single-axis tracking and flat-plate collector without tracking during cloudy-sky days," *Sol. Energy*, vol. 291, p. 113412, 2025. https://doi.org/10.1016/j.solener.2025.113412

[12] M. N. Hussain, M. A. Halim, M. Y. A. Khan, S. Ibrahim, and A. Haque, "A comprehensive review on techniques and challenges of energy harvesting from distributed renewable energy sources for wireless sensor networks," *Control Syst. Optim. Lett.*, vol. 2, no. 1, pp. 15–22, 2024. https://doi.org/10.59247/csol.v2i1.60

[13] P. Roth, A. Georgiev, and H. Boudinov, "Design and construction of a system for sun-tracking," *Renew. Energy*, vol. 29, no. 3, pp. 393–402, 2004. https://doi.org/10.1016/S0960-1481(03)00196-4

[14] A. B. Sproul, "Derivation of the solar geometric relationships using vector analysis," *Renew. Energy*, vol. 32, no. 7, pp. 1187–1205, 2007. https://doi.org/10.1016/j.renene.2006.05.001

[15] E. M. H. Arif, J. Hossen, G. Ramana, T. Bhuvaneswari, P. Velrajkumar, and C. Venkataseshaiah, "A survey on neuro-fuzzy controllers for solar panel tracking systems," *Far East J. Electron. Commun.*, vol. 18, no. 7, pp. 981–1003, 2018. https://doi.org/10.17654/EC018070981

[16] A. Musa, E. Alozie, S. A. Suleiman, J. A. Ojo, and A. L. Imoize, "A review of time-based solar photovoltaic tracking systems," *Information*, vol. 14, no. 4, p. 211, 2023. https://doi.org/10.3390/info14040211

[17] R. C. Neville, "Solar energy collector orientation and tracking mode," *Sol. Energy*, vol. 20, no. 1, pp. 7–11, 1978. https://doi.org/10.1016/0038-092X(78)90134-2

[18] P. Drago, "A simulated comparison of the useful energy gain in a fixed and a fully tracking flat plate collector," *Sol. Energy*, vol. 20, no. 5, pp. 419–423, 1978. https://doi.org/10.1016/0038-092X(78)90160-3

[19] T. Tomson and G. Tamm, "Performance of flat-plate collectors with two-positional active tracking," *Proc. Estonian Acad. Sci. Eng.*, vol. 13, no. 1, pp. 26–36, 2007.

[20] T. Tomson, "Discrete two-positional tracking of solar collectors," *Renew. Energy*, vol. 33, no. 3, pp. 400–405, 2008. https://doi.org/10.1016/j.renene.2007.03.017

[21] C. B. Maia, A. G. Ferreira, and S. M. Hanriot, "Evaluation of a tracking flat-plate solar collector in Brazil," *Appl. Therm. Eng.*, vol. 73, no. 1, pp. 953–962, 2014. https://doi.org/10.1016/j.applthermaleng.2014.08.052

[22] J. D. Garrison, "A program for calculation of solar energy collection by fixed and tracking collectors," *Sol. Energy*, vol. 73, no. 4, pp. 241–255, 2002. https://doi.org/10.1016/S0038-092X(02)00066-X

[23] W. F. Marion and A. P. Dobos, "Rotation angle for the optimum tracking of one-axis trackers," National Renewable Energy Laboratory, Technical Report NREL/TP-6A20-58891, 2013.

[24] A. Aghamohammadi and M. E. Foulaadvand, "Efficiency comparison between tracking and optimally fixed flat solar collectors," *Sci. Rep.*, vol. 13, no. 1, p. 12712, 2023. https://doi.org/10.1038/s41598-023-39892-y

[25] A. Bahrami, C. O. Okoye, H. H. Pourasl, and V. M. Khojastehnezhad, "Techno-economic comparison of fixed and tracking flat plate solar collectors in the northern hemisphere," *J. Clean. Prod.*, vol. 378, p. 134523, 2022. https://doi.org/10.1016/j.jclepro.2022.134523

[26] H. D. Kambezidis, K. A. Kavadias, and A. M. Farahat, "Solar energy received on flat-plate collectors fixed on 2-axis trackers: Effect of ground albedo and clouds," *Energies*, vol. 17, no. 15, p. 3721, 2024. https://doi.org/10.3390/en17153721

[27] M. Neagoe, I. Visa, B. G. Burduhos, and M. D. Moldovan, "Thermal load based adaptive tracking for flat plate solar collectors," *Energy Procedia*, vol. 48, pp. 1401–1411, 2014. https://doi.org/10.1016/j.egypro.2014.02.158

[28] M. Chekerovska and R. V. Filkoski, "Efficiency of liquid flat-plate solar energy collector with solar tracking

system," *Therm. Sci.*, vol. 19, no. 5, pp. 1673–1684, 2015. https://doi.org/10.2298/TSCI150427099C
[29] I. Ajunwa, D. S. Yawas, D. M. Kulla, M. B. Abdullahi, I. U. Ibrahim, and M. Iorpenda Jnr., "Performance improvement of an indirect solar dryer with single axis manual tracking system and angular simulation of the flat plate collector reflectors," *Arid Zone J. Eng. Technol. Environ.*, vol. 16, no. 2, pp. 293–308, 2020.
[30] A. M. Nešović, N. S. Lukić, M. M. Josijević, N. M. Jurišević, and N. N. Nikolić, "Novel flat-plate solar collector with an inclined N-S axis and relative E-W tracking absorbers and the numerical analysis of its potentials," *Therm. Sci.*, vol. 28, no. 4, pp. 2905–2916, 2024. https://doi.org/10.2298/TSCI230201115N
[31] A. Nešović, "Numerical analysis of the total incident solar radiation on the flat-plate solar collector with single-axis tracking–case with inclined N-S axis and E-W tracking," 2022, University of Kragujevac Digital Archive, University of Kragujevac, Serbia. https://scidar.kg.ac.rs/handle/123456789/18757
[32] D. Z. Djurdjevic, "Perspectives and assessments of solar PV power engineering in the Republic of Serbia," *Renew. Sust. Energ. Rev.*, vol. 15, no. 5, pp. 2431–2446, 2011. https://doi.org/10.1016/j.rser.2011.02.025
[33] Climate.OneBuilding.Org, "Repository of building simulation climate data," 2025. https://climate.onebuilding.org/
[34] SketchUp, "Google SketchUp software," 2025. https://www.sketchup.com/en
[35] EnergyPlus, "EnergyPlus software," 2025. https://energyplus.net/
[36] D. B. Crawley, L. K. Lawrie, C. O. Pedersen, and F. C. Winkelmann, "EnergyPlus: Energy simulation program," *Ashrae J.*, vol. 42, no. 4, pp. 49–56, 2000.
[37] L. E. Hartley, J. A. Martínez-Lozano, M. P. Utrillas, F. Tena, and R. Pedros, "The optimisation of the angle of inclination of a solar collector to maximise the incident solar radiation," *Renew. Energy*, vol. 17, no. 3, pp. 291–309, 1999. https://doi.org/10.1016/S0960-1481(98)00763-0
[38] T. Tesfamichael and E. Wäckelgård, "Angular solar absorptance and incident angle modifier of selective absorbers for solar thermal collectors," *Sol. Energy*, vol. 68, no. 4, pp. 335–341, 2000. https://doi.org/10.1016/S0038-092X(00)00029-3

Nomenclature

c	speed, $\mathrm{m.s^{-1}}$
H	terrestrial solar radiation, $\mathrm{W.m^{-2}}$
I	incident solar radiation, W and W. day $^{-1}$
t	temperature, °C

Greek symbols

α	altitude angle, $^\circ$
β	inclination angle, $^\circ$
λ	longitude, $^\circ$
φ	latitude, $^\circ$
ψ	rotation step and rotation angle, $^\circ$

Subscripts

beam	beam
cr	circumsolar region
diff	diffuse
fix	fixed surface
max	maximum
min	minimum
o	air
refl	reflected
sh	sky horizon
sk	sky dome
tot	total
w	wind

Abbreviation

DAT dual	axis tracking
FPSC flat	plate solar collector
SAT single	axis tracking